frontiers in Materials

ORIGINAL RESEARCH
published: 30 April 2021
doi: 10.3389/fmats.2021.649998

TiO_2 Nanowire Arrays *in situ* Grown on Ti Foil Exhibiting Superior Uranyl-Adsorption Properties

Chun Chen, Yi Zhong, Xuxu Liu, Xijian Li, Jian Chu, Libing Yu, Zhenliang Yang, Bingqing Li, Wei Tang, Zhonghua Xiong and Rui Gao**

Institute of Materials, China Academy of Engineering Physics, Mianyang, China

OPEN ACCESS

Edited by:
P. Davide Cozzoli, University of Salento, Italy

Reviewed by:
Ali Azari, Kashan University of Medical Sciences, Iran
Xiangke Wang, North China Electric Power University, China
Imran Ali, Jamia Millia Islamia, India

***Correspondence:**
Zhonghua Xiong
xiongzhonghua@caep.cn
Rui Gao
gaor04@126.com

Specialty section:
This article was submitted to Colloidal Materials and Interfaces, a section of the journal Frontiers in Materials

Received: *07 January 2021*
Accepted: *01 March 2021*
Published: *30 April 2021*

Citation:
Chen C, Zhong Y, Liu X, Li X, Chu J, Yu L, Yang Z, Li B, Tang W, Xiong Z and Gao R (2021) TiO_2 Nanowire Arrays in situ Grown on Ti Foil Exhibiting Superior Uranyl-Adsorption Properties. Front. Mater. 8:649998. doi: 10.3389/fmats.2021.649998

TiO_2 nanowire arrays *in situ* grown on Ti foil (TiO_2/Ti) were prepared to remove uranium (VI) from aqueous solution. As the Ti foil serves as a carrier for TiO_2, the TiO_2/Ti adsorbent can be effortlessly retrieved from aqueous solutions by tweezers after adsorption. The presence of TiO_2 nanowire arrays on Ti foil was verified by X-ray diffraction and scanning electron microscopy. Parameters in the adsorption process were fully evaluated, including solution pH, contact time, temperature, and uranium (VI) concentration. The adsorption was most efficient in the pH range of 5.0 to 9.0. The maximum uranium (VI) adsorption capacity of TiO_2/Ti, based on the Langmuir model, was 354.5 mg g^{-1} at pH 5.0 and T = 323 K. Thermodynamic parameters showed that the adsorption of uranium (VI) on TiO_2/Ti is endothermic and spontaneous. The adsorption capacity of TiO_2/Ti remained essentially unchanged after three adsorption–desorption cycles in uranium (VI) solutions. Our results support the application of this adsorbent to removal of uranium (VI) from diversified aqueous samples.

Keywords: uranyl, TiO_2, nanowire, Ti foil, adsorption, *in situ* growth, reusability

INTRODUCTION

With the rapid development of nuclear power, environmental pollution by uranium has raised global concerns. For example, uranium mining and hydrometallurgical processes are known to cause serious water contamination. Uranium contamination is harmful and long-lasting because of its radiotoxicity and chemotoxicity (Basheer, 2018a,b). The potential radiation damage and chemotoxicity of uranium pose serious threats to human health (Kurttio et al., 2006; Prat et al., 2009; Schnug and Lottermoser, 2013; Manigandan and Chandar Shekar, 2014). Meanwhile, uranium resources for nuclear power face potential depletion in the near future and cannot meet the urgent industrial demands. Therefore, the removal and recovery of uranium from waste and natural water are critically important for environmental protection and conservation of energy resources (Xie et al., 2019). Conventional methods for the treatment of water containing uranium include chemical precipitation, adsorption, solvent extraction, electrocoagulation, membrane filtration, and biological methods (Shi et al., 2009; Santos and Ladeira, 2011; Stylo et al., 2013; Tripathi et al., 2013; Azari et al., 2014, 2017, 2019; Beltrami et al., 2014; Karami et al., 2017; Li et al., 2017; Zhu et al., 2019; Zhong et al., 2021). Among various methods, adsorption techniques are relatively efficient, cost-effective, and easy to

implement, exhibiting great potential for removing uranium (VI) from aqueous solutions (Ali et al., 2019; Xie et al., 2019; Azari et al., 2020; Liu et al., 2021).

To date, assorted types of adsorbents have been developed for uranium, such as activated carbon, oxides, graphene, nanocomposites, and polymers (Nair et al., 2014; Xu et al., 2015; Zhang et al., 2015; Wang et al., 2016; El-Maghrabi et al., 2017). Among these adsorbents, metal oxides, especially titanium dioxide, have attracted considerable attention because of its high adsorptive capacity for uranium (VI), good radiochemical stability, and negligible solubility in both acidic and alkaline solutions (Comarmond et al., 2011; Tatarchuk et al., 2019; Wang et al., 2019). However, the separation of TiO_2-based adsorbents from aqueous solutions after adsorption is usually complicated and time-consuming. To solve this problem, methods based on external magnetic field or coprecipitation have been explored (Tan et al., 2015; Wen et al., 2018).

In this study, we prepared TiO_2 nanowire arrays (NWAs) on Ti foil (TiO_2/Ti) via *in situ* growth. The TiO_2 nanowires provide abundant active surface sites for uranium adsorption. The Ti foil serves as a carrier for TiO_2 and can be removed from the solution with tweezers, achieving simple and effective separation of the adsorbent. The chemical components and structure of TiO_2/Ti were characterized by X-ray diffraction (XRD) and scanning electron microscope (SEM), and the uranium (VI) adsorption process by TiO_2/Ti was comprehensively evaluated. The results reveal that the TiO_2/Ti adsorbent has superior uranium adsorption capacity (VI) and excellent reusability.

MATERIALS AND METHODS

Ti foil, NaOH, HCl, ethanol, and sodium citrate were purchased from Alfa Aesar. The purity of Ti foil is > 99.9%, and other reagents are analytically pure. Uranyl nitrate was provided by Dingtian Chem. Corp. (Xi'an). All chemical reagents were used without further purification.

The fabrication method of TiO2 NWAs on Ti foil is as follows. A piece of Ti foil was ultrasonically cleaned in deionized (DI) water for 10 min and in ethanol for 10 min. It was placed in a 50-mL Teflon-lined stainless-steel autoclave with 30 mL 1 M NaOH and 0.01 M sodium citrate aqueous solution. The hydrothermal reaction was performed at 220°C for 24 h. The Ti foil covered with TiO_2 NWA was immersed in 1 M HCl solution for 5 min to replace Na^+ with H^+. Then, the Ti foil with TiO_2 NWAs was rinsed with DI water and ethanol. Finally, the obtained TiO_2/Ti was sintered at 450°C for 30 min.

In a typical adsorption experiment, a given amount of TiO_2/Ti was mixed with 20 mL $UO_2(NO_3)_2{\cdot}6H_2O$ solution in a conical flask. The conical flask was placed in a thermostatic water shaker at a speed of 150 revolutions/min. In this process, the experimental parameters were adjusted, including solution concentration, solution pH, adsorption time, and temperature. The solution pH was adjusted by adding 0.1 M HNO_3 or NaOH solution. After the adsorption processes, the ^{VI}U-TiO_2/Ti samples were collected with tweezers. The adsorption capacity (Q_e) and adsorption removal efficiency were calculated according to the following equations (Tan et al., 2015):

$$Q_e = \frac{(C_0 - C_e)V}{m} \tag{1}$$

$$\text{Removal}\,(\%) = \frac{100\,(C_0 - C_e)}{C_0} \tag{2}$$

where, C_0 and C_e (mg L^{-1}) are concentrations of uranium (VI) at the initial and equilibrium states, respectively; m (g) is the weight of TiO_2/Ti adsorbent, and V (L) is the volume of the solution. The distribution coefficient (K_D) was obtained according to Eq. (3) (Wang et al., 2019):

$$K_D = \frac{C_0 - C_e}{C_e} \times \frac{V}{m} \tag{3}$$

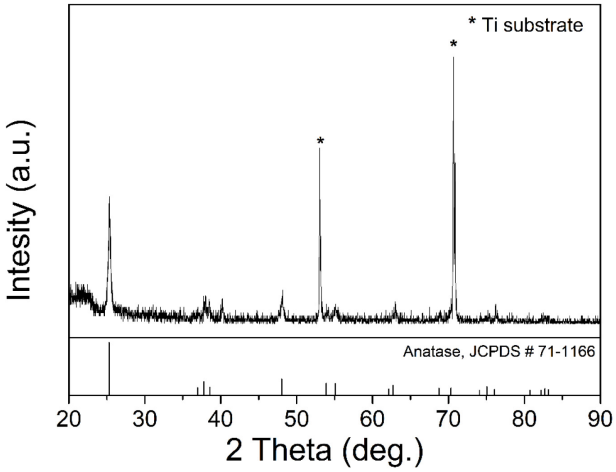

FIGURE 1 | XRD pattern of TiO_2/Ti. *Peaks of Ti.

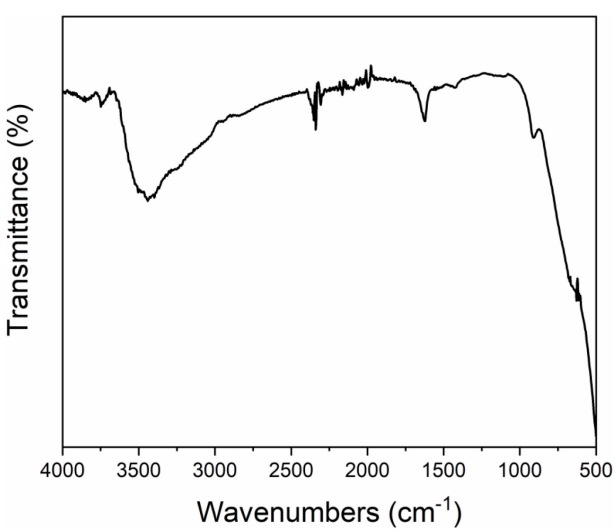

FIGURE 2 | FTIR spectrum of TiO_2/Ti.

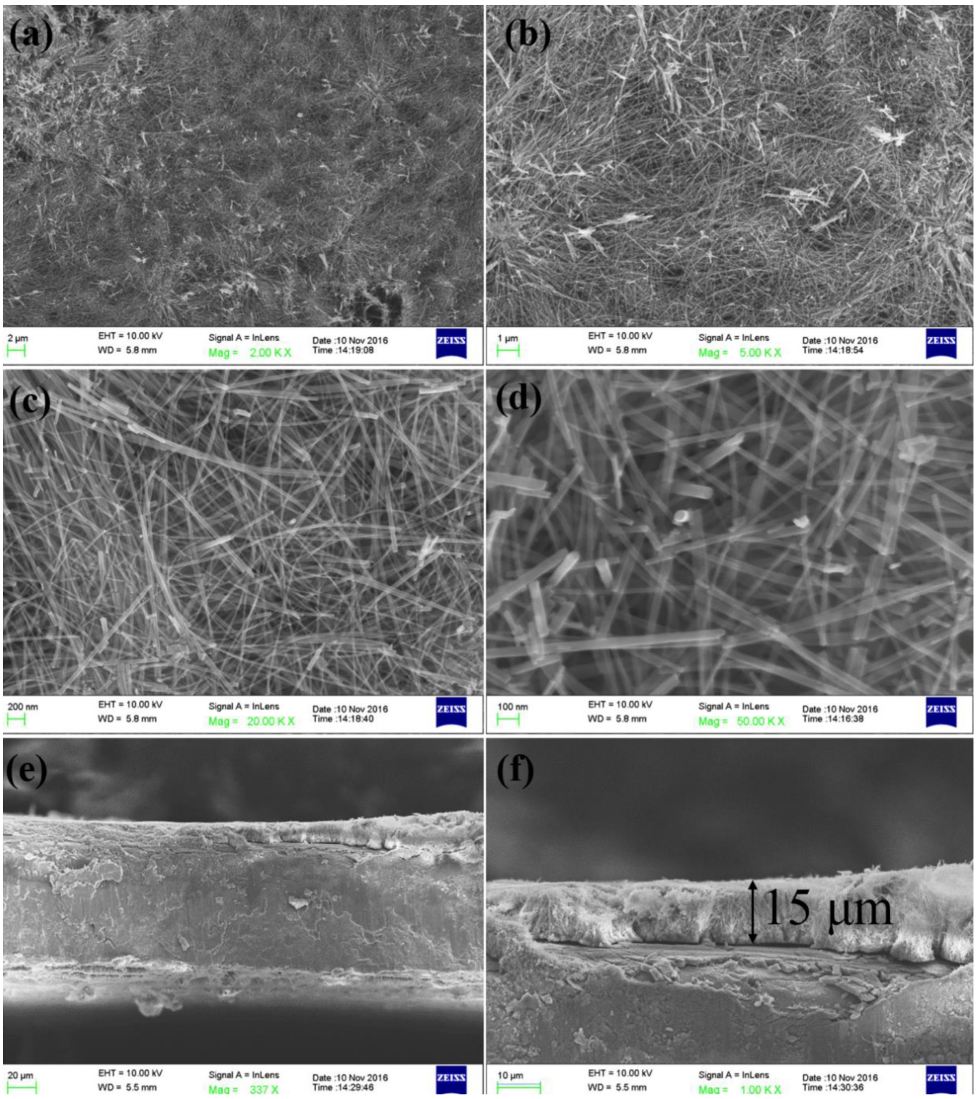

FIGURE 3 | (a–f) Are all SEM images of TiO_2/Ti. Oriented TiO_2 NWAs are assembled on the Ti foil.

The phase constitution of TiO_2/Ti was analyzed by XRD on a Tongda TD-3500 diffractometer at a scanning rate of 4°/min. The microstructure was studied by an SEM (Helios NanoLab 600i, ZEISS).

Desorption was carried out by soaking the ^{VI}U-TiO_2/Ti samples in 20 mL 0.1 mol L^{-1} HCl solution for 60 min, followed by thorough washing with DI water. The desorbed TiO_2/Ti adsorbents were then reused.

RESULTS AND DISCUSSION

Characterization of Samples

The XRD patterns of TiO_2/Ti are shown in **Figure 1**. All characteristic peaks of TiO_2 were observed (Anatase, JCPDS #71-1166). The peaks of Ti were marked with stars in **Figure 1**. This result indicated successful fabrication of crystalline TiO_2 on the Ti foil. As shown in **Figure 2**, the peaks that appeared in 600 and 1,040 cm^{-1} were Ti-O bending vibration, which further proved the TiO_2 has been successfully fabricated. The broad bands in the range of 3,000–3,600 cm^{-1} and 1,600–1,645 cm^{-1} were H–O–H bending vibration. It indicated that the fabricated TiO_2 nanowires adsorbed water while they were exposed to the air. In **Figure 3**, homogenous TiO_2 NWAs were observed on the Ti foil. The length of TiO2 NWs is greater than 10 μm, and the thickness of the TiO2 film on Ti foil substrate is approximately 15 μm. The large specific surface area can potentially provide superior adsorption performance.

Effect of Solution pH

Solution pH plays an important role in the adsorption process owing to its influences on the aqueous chemical properties of

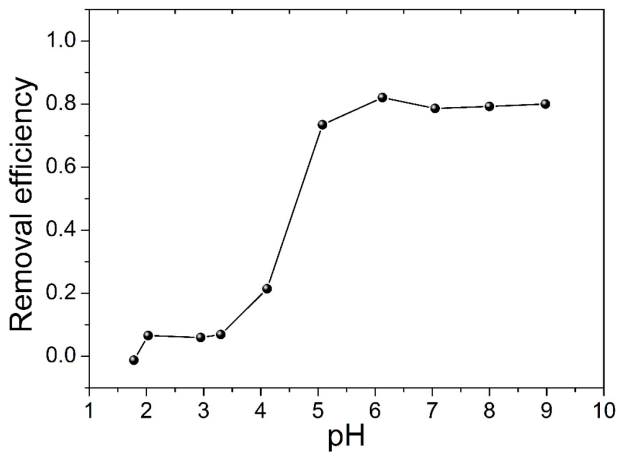

FIGURE 4 | Effect of pH on the removal of uranium (VI) (C_0 = 8 mg L^{-1}, t = 1 h, T = 298 K).

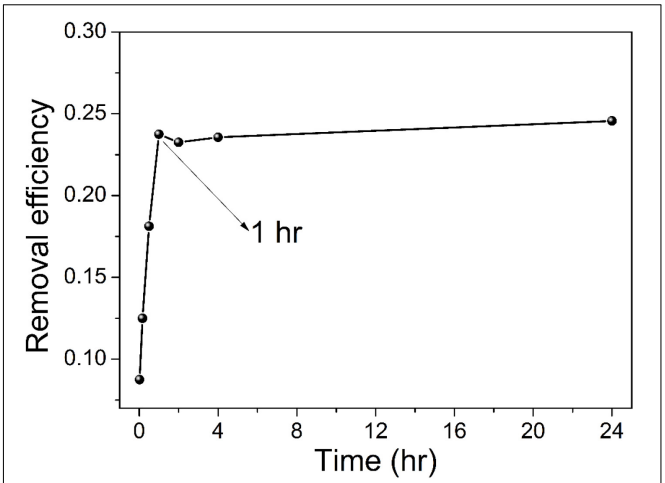

FIGURE 5 | The relationship between uranium removal efficiency by TiO_2/Ti and contact time (T = 298 K, pH 5.0, C_0 = 40 mg L^{-1}, mixing time 1–1,440 min, and amount of TiO_2/Ti 0.025 g).

uranium and the adsorbent (Lamb et al., 2016; Song et al., 2017). **Figure 4** depicts the effect of initial pH in aqueous solution on uranium (VI) removal efficiency. The removal of uranium (VI) by TiO_2/Ti was tested by varying pH from 1.5 to 9.0. The removal efficiency sharply increased as pH increased from 3.0 to 5.0 and remained almost unchanged from 5.0 to 9.0. At pH < 3.0, the binding sites on TiO_2/Ti surface become positively charged, and the adsorption of uranyl cations is negligible. At pH > 3.0, the surface of TiO_2/Ti becomes deprotonated, resulting in sharp increase of uranium (VI) adsorption. Further increase in pH may lead to the formation of anionic uranyl complexes, which suppress the adsorption of uranium (VI) onto TiO_2/Ti materials (Tatarchuk et al., 2019; Wang et al., 2019).

Effect of Contact Time and Adsorption Dynamics

Figure 5 shows the effect of contact time on uranium (VI) removal by TiO_2/Ti. Contact times from 5 min to 24 h were evaluated.

As shown in **Figure 5**, uranium (VI) removal increases with the increase of contact time, and the adsorption process reaches equilibrium after 1 h. To probe the kinetic mechanism of uranium adsorption on TiO_2/Ti, the adsorption data were analyzed using pseudo–first-order and pseudo–second-order models. The pseudo–first-order and pseudo–second-order kinetic equations are (Ho and McKay, 1999; Ho, 2006):

$$\ln (Q_e - Q_t) = \ln Q_e - k_1 t \tag{4}$$

$$\frac{t}{Q_t} = \frac{1}{k_2 Q_e^2} + \frac{t}{Q_e} \tag{5}$$

where, k_1 (min^{-1}) represents the pseudo–first-order adsorption rate constant, t (min) is time. Q_e and Q_t (mg g^{-1}) are adsorption capacity of uranium at equilibrium and at time t, respectively. k_2 (g mg^{-1} min^{-1}) is the pseudo–second-order adsorption rate constant. The pseudo-first-order and pseudo-second-order fitting curves are shown in **Figures 6A,B**, respectively. The relevant kinetics data are presented in **Table 1**. The adsorption of uranium (VI) on TiO_2/Ti more likely follows the pseudo–second-order model (R^2 = 0.99) than the pseudo–first-order model (R^2 = 0.39). The pseudo–second-order kinetic model further indicates that the dominant mechanism for uranium (VI) adsorption on TiO_2/Ti is chemical adsorption or strong surface complexation rather than mass transport (Ho and McKay, 2000; Kamari et al., 2009).

Adsorption Isotherms of Uranium

According to **Figure 7**, the adsorption capacity increases with elevating temperature. The adsorption data were analyzed using the Langmuir and Freundlich isotherm models (Freundlich, 1906; Langmuir, 1918). The linearized form of the Langmuir equation is:

$$\frac{C_e}{Q_e} = \frac{1}{K_L Q_m} + \frac{C_e}{Q_m} \tag{6}$$

where, K_L (L mg^{-1}) is the Langmuir constant; Q_e and Q_m (mg g^{-1}) are the equilibrium adsorption capacity and maximum adsorption capacity, respectively. Q_m and K_L can be calculated from the linear regression of C_e/Q_e against C_e (**Figure 8A**).

The Freundlich isotherm is applicable to the adsorption on heterogeneous surfaces and multilayer adsorption. The linear form of Freundlich isotherm is:

$$\ln Q_e = \ln K_F + \frac{1}{n} \ln C_e \tag{7}$$

where, K_F is the Freundlich constant, and n is adsorption intensity. K_F and n constants can be calculated from the linear regression of $\ln Q_e$ versus $\ln C_e$ (**Figure 8B**).

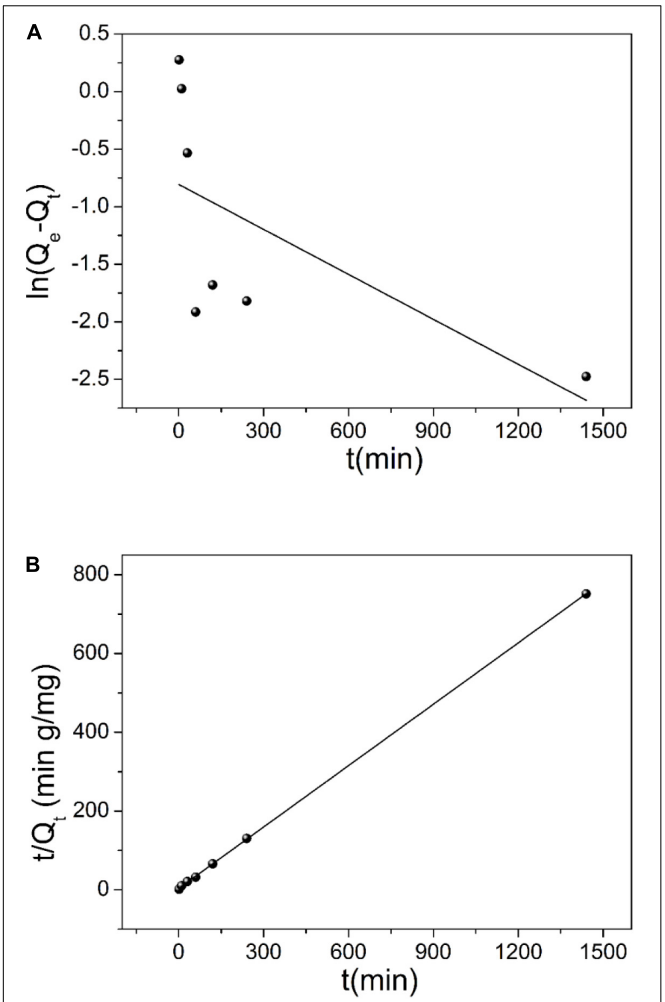

FIGURE 6 | The fitting of pseudo–first-order **(A)** and pseudo–second-order **(B)** kinetic models for uranium (VI) adsorption on TiO_2/Ti.

TABLE 1 | Kinetic parameters of different models for uranium (VI) adsorption on TiO_2/Ti (temperature 298 K, pH 5.0, mixing time 60 min, and amount of TiO_2/Ti 0.025 g).

Kinetic model	T (K)	C_0 (mg L^{-1})	Q_{cal} (mg g^{-1})	k_1 (min^{-1}) k_2 (g•mg min^{-1})	R^2
Pseudo–first-order	298	40	—	—	0.392
Pseudo–second-order	298	40	192.4	0.137	0.999

The parameters of Langmuir and Freundlich equations are summarized in **Table 2**. The correlation coefficients (R^2) indicate that the Langmuir model better accounts for the behavior of uranium (VI) adsorption by TiO_2/Ti. According to the Langmuir isotherm, the monolayer saturation capacity of TiO_2/Ti is about 354.5 mg g^{-1} for uranium (VI) at 323 K. The comparison of uranium (VI) adsorption capacity onto different TiO_2 and its composites at 298 K is listed in **Table 3**.

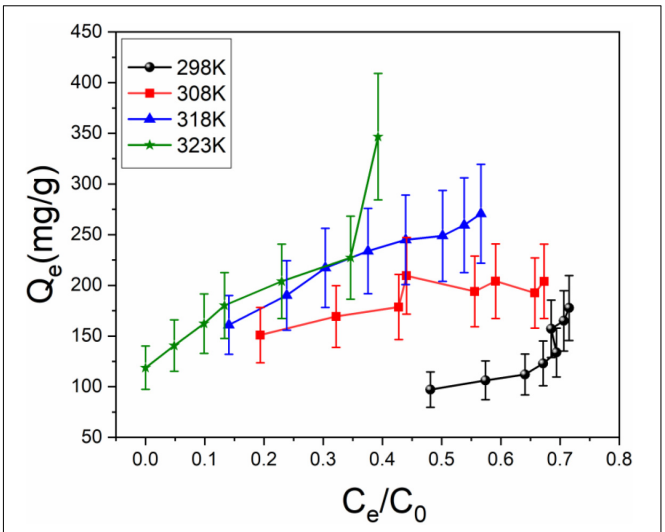

FIGURE 7 | Adsorption isotherms of TiO_2/Ti for uranium (VI) at different temperatures (temperature 298–323 K, pH 5.0, amount of TiO_2/Ti 0.025 g, and mixing time 60 min).

Effect of Temperature and Adsorption Thermodynamics

The effect of temperature on the uranium (VI) adsorption by TiO_2/Ti was investigated at 298, 308, 318, and 323 K. Based on **Figure 7** and **Table 2**, the adsorption capacity of uranium (VI) increases from 204.2 to 354.5 mg g^{-1} as the temperature rises from 298 to 323 K, suggesting that higher temperature is advantageous for uranium (VI) adsorption.

To understand the thermodynamic aspect of the adsorption process, the standard free energy change ($\Delta G°$), standard enthalpy change ($\Delta H°$), and standard entropy change ($\Delta S°$) are calculated from the adsorption data at different temperatures via the following equations:

$$\ln K_D = -\frac{\Delta H°}{RT} + \frac{\Delta S°}{R} \tag{8}$$

$$\Delta G° = \Delta H° - T\Delta S° \tag{9}$$

where, K_D is the distribution coefficient (mL g^{-1}), R is the ideal gas constant (8.314 J mol^{-1} K^{-1}), and T is the temperature (K). The $\Delta H°$ and $\Delta S°$ values are determined from the slope and intercept of the linear regression of $\ln K_D$ versus $1/T$, respectively (**Figure 9**). The thermodynamic parameters are in **Table 4**. The positive $\Delta H°$ indicates an endothermic adsorption process of uranium on TiO_2/Ti. The negative $\Delta G°$ indicates a spontaneous adsorption process. Moreover, the absolute value of $\Delta G°$ increases with elevating temperature, suggesting higher temperature is conducive to the adsorption of metal ions. The positive $\Delta S°$ indicates an increase of randomness on the adsorbent surface during the adsorption process. Therefore, the adsorption of uranium (VI) on TiO_2/Ti is endothermic and spontaneous.

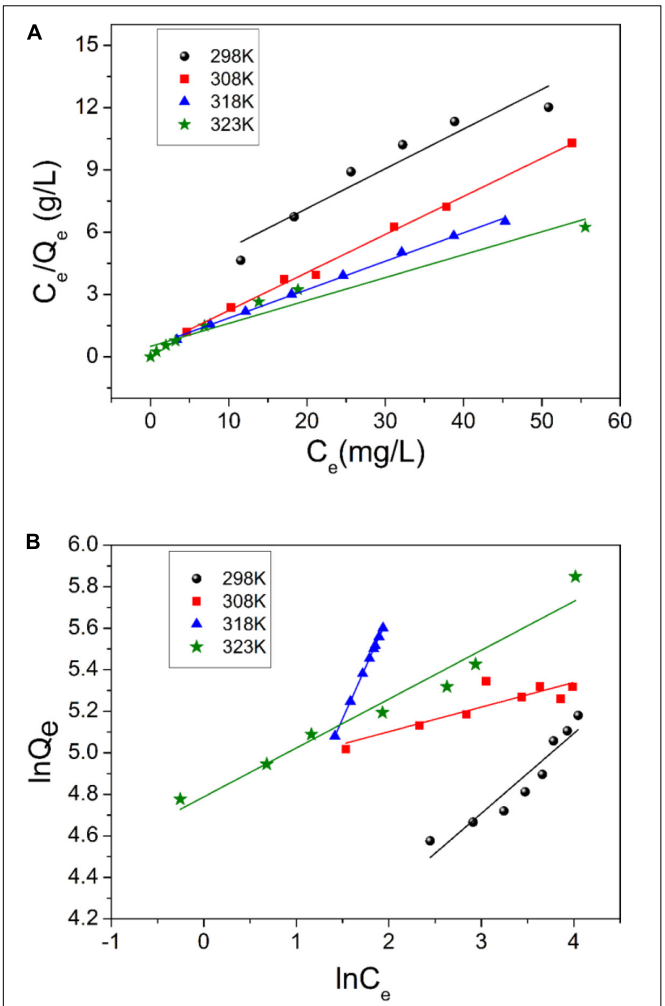

FIGURE 8 | Langmuir **(A)** and Freundlich **(B)** plot for the adsorption of uranium (VI) on TiO_2/Ti (temperature 298–323 K, pH 5.0, amount of TiO_2/Ti 0.025 g, and mixing time 60 min).

TABLE 3 | The comparison of uranium (I) adsorption capacity onto different TiO_2 and its composites at 298 K.

Adsorbent	Adsorption capacity (mg g^{-1})	References
TiO_2	11.4	Wang et al., 2019
Fe_3O_4@TiO_2	91	Tan et al., 2015
β-zeolite@TiO_2	34	Peng et al., 2017
Wool-AO@TiO_2	113.12	Wen et al., 2018
CeO_2-TiO_2-Fe_2O_3	440	El-sherif et al., 2017
TiO_2/Ti	204.2	This work

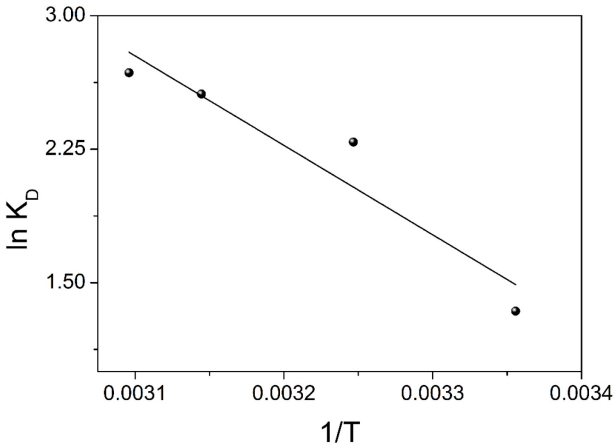

FIGURE 9 | Linear regression of lnK_D and 1/T.

TABLE 4 | Thermodynamic parameters for uranium adsorption on TiO_2/Ti.

$\Delta H°$ (kJ mol^{-1})	$\Delta S°$ (J $mol^{-1}·K^{-1}$)	$\Delta G°$ (kJ mol^{-1})			
41.8	152.1	298K	308K	318K	323K
		−3.52	−5.04	−6.56	−7.32

TABLE 2 | Isotherm constants and values of R^2 for TiO_2/Ti.

T (K)	Langmuir constants			Freundlich constants		
	Q_m (mg g^{-1})	K_L (L g^{-1})	R^2	K_F (L g^{-1})$^{1/n}$	1/n	R^2
298	204.2	1.48	0.900	34.88	0.385	0.889
308	213.1	11.79	0.996	129.7	0.118	0.736
318	284.7	7.17	0.997	39.0	1.000	1.000
323	354.5	5.58	0.947	120.0	0.235	0.952

Desorption and Reusability Study

We performed two desorption experiments to assess the reusability of TiO_2/Ti adsorbent. First, as depicted in **Scheme 1**, 20 mL uranium (VI) solution was used as the target solution. A piece of TiO_2/Ti was immersed in the target solution for 60 min. After adsorption, the adsorbents were removed from the solution with tweezers and treated with 0.1 mol L^{-1} HCl solution for 60 min. Then, the desorbed TiO_2/Ti adsorbents were reused in an identical target solution. The above adsorption–desorption cycle was repeated nine times. The initial uranium (VI) amount exceeded the maximum adsorption capacity of TiO_2/Ti. The adsorption capacity of uranium (VI) and the residual uranium (VI) in target solution after every cycle were recorded. As shown in **Figure 10**, the adsorption capacity (Q_e) was approximately 355 mg g^{-1} in the first cycle and decreased to 45 mg g^{-1} in the ninth time. This could be attributed to the continuous decrease of uranium (VI) concentration after each adsorption cycle. The residual uranium (VI) in the target solution was approximately 8% after nine cycles.

Second, three identical uranium (VI) solutions (I, II, and III) were tested with the same piece of TiO_2/Ti. It was first immersed in solution I for 60 min. After adsorption, it was retrieved from the solution with tweezers and treated with 0.1 mol L^{-1} HCl solution for 60 min. Next, the

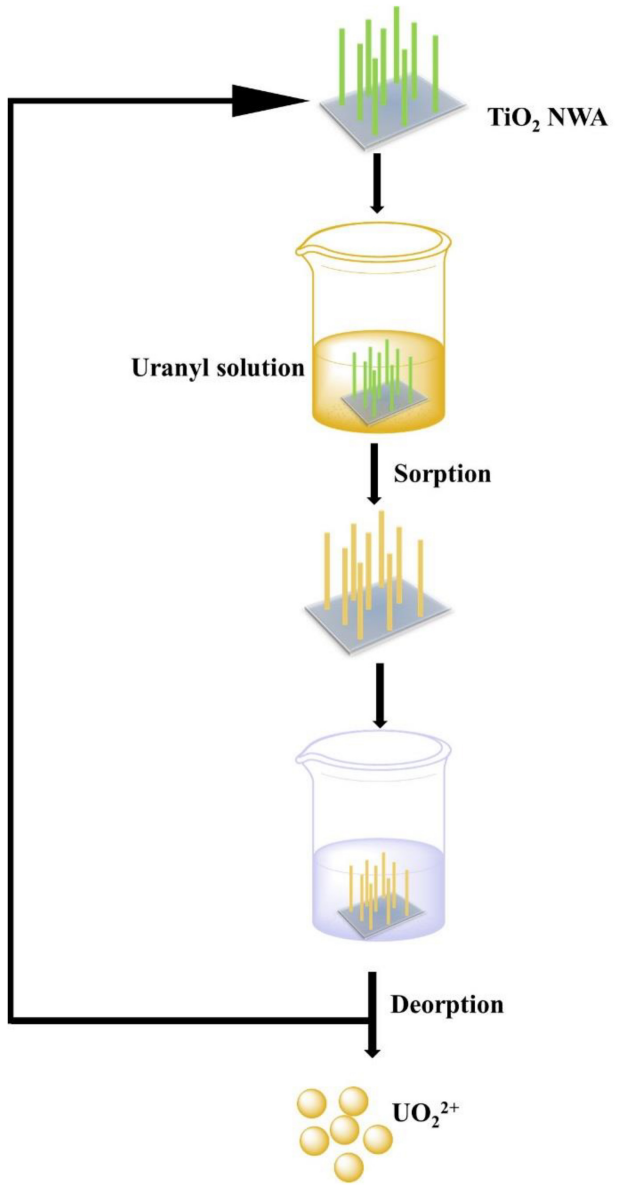

SCHEME 1 | The adsorption–desorption process of TiO_2 nanowires grown on Ti foil.

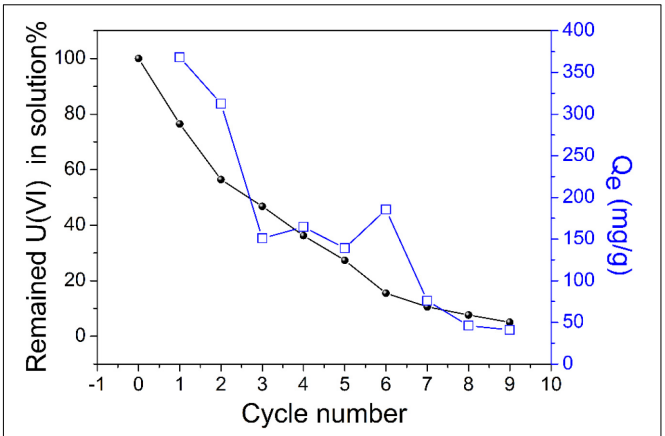

FIGURE 10 | The reusability of TiO_2/Ti adsorbents in the target solution (temperature 298 K, pH 5.0, amount of TiO_2/Ti 0.025 g, mixing time 60 min, and C_0 = 200 mg L^{-1}).

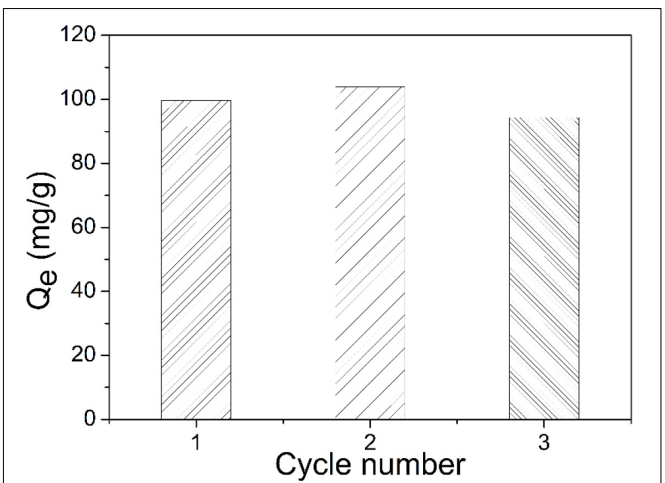

FIGURE 11 | The reusability of TiO_2/Ti adsorbents evaluated in three identical uranium solutions (temperature 303 K, pH 5.0, amount of TiO_2/Ti 0.025 g, mixing time 60 min, and C_0 = 100 mg L^{-1}).

recovered TiO_2/Ti piece underwent the same adsorption–desorption procedure in solution II and then in solution III. According to **Figure 11**, the adsorption capacity (Q_e) of TiO_2/Ti remained essentially unchanged during three successive adsorption cycles.

CONCLUSION

TiO_2 NWAs *in situ* grown on Ti foil were constructed to recover uranium (VI) from aqueous solutions. The uranium (VI) adsorption capacity was affected by solution pH, contact time, temperature, and uranium (VI) concentration. The adsorption was most efficient in the pH range of 5.0 to 9.0. The adsorption process was found to follow pseudo–second-order kinetics and the Langmuir model, and the maximum uranium (VI) adsorption capacity was 354.5 mg g^{-1}. Thermodynamic parameters suggest that the adsorption of uranium (VI) on TiO_2/Ti is endothermic and spontaneous. Meanwhile, the TiO_2/Ti material showed remarkable reusability, effectively removing 92% uranium (VI) after nine adsorption cycles. In addition, the TiO_2/Ti adsorbents can be rapidly retrieved from aqueous solutions by tweezers. The ease of operation, superior adsorption performance, and excellent reusability indicate that the TiO_2/Ti adsorbent could be potentially applied to the removal of uranium (VI) from water in diverse practical applications.

DATA AVAILABILITY STATEMENT

The original contributions presented in the study are included in the article/supplementary material, further inquiries can be directed to the corresponding author/s.

AUTHOR CONTRIBUTIONS

CC contributed to data curation, writing—original draft preparation, and funding acquisition. YZ and XuL contributed to investigation. XiL, JC, LY, ZY, BL, and WT contributed to conceptualization and investigation. ZX contributed to supervision and conceptualization. RG contributed to validation, writing, reviewing, and editing. All authors contributed to the article and approved the submitted version.

ACKNOWLEDGMENTS

This work was supported by the National Natural Science Foundation of China [Nos. 21703214 and 22006140].

REFERENCES

Ali, I., Burakov, A. E., Melezhik, A. V., Babkin, A. V., Burakova, I. V., Neskomornaya, E. A., et al. (2019). Removal of Copper(II) and Zinc(II) Ions in Water on a Newly Synthesized Polyhydroquinone/Graphene Nanocomposite Material: Kinetics, Thermodynamics and Mechanism. . *ChemistrySelect* 4, 12708–12718. doi: 10.1002/slct.201902657

Azari, A., Babaie, A. A., Rezaei-Kalantary, R., Esrafili, A., and Kakavandi, B. (2014). Nitrate removal from aqueous solution by carbon nanotubes magnetized with nano zero-valent iron. *J. Mazandaran Univ. Med. Sci.* 23, 15–27.

Azari, A., Nabizadeh, R., Nasseri, S., Mahvi, A. H., and Mesdaghinia, A. R. (2020). Comprehensive systematic review and meta-analysis of dyes adsorption by carbon-based adsorbent materials: Classification and analysis of last decade studies. *Chemosphere* 250, 126238. doi: 10.1016/j.chemosphere.2020.126238

Azari, A., Noorisepehr, M., Dehghanifard, E., Karimyan, K., Hashemi, S. Y., Kalhori, E. M., et al. (2019). Experimental design, modeling and mechanism of cationic dyes biosorption on to magnetic chitosan-lutaraldehyde composite. *Int. J. Biol. Macromol* 131, 633–645. doi: 10.1016/j.ijbiomac.2019.03.058

Azari, A., Salari, M., Dehghani, M. H., Alimohammadi, M., Ghaffari, H., Sharafi, K., et al. (2017). Efficiency of Magnitized Graphene Oxide Nanoparticles in Removal of 2,4-Dichlorophenol from Aqueous Solution. *J. Mazandaran Univ. Med. Sci.* 26, 265–281.

Basheer, A. A. (2018a). Chemical chiral pollution: Impact on the society and science and need of the regulations in the 21st century. *Chirality* 30, 402–406. doi: 10.1002/chir.22808

Basheer, A. A. (2018b). New generation nano-adsorbents for the removal of emerging contaminants in water. *Journal of Molecular Liquids* 261, 583–593. doi: 10.1016/j.molliq.2018.04.021

Beltrami, D., Cote, G., Mokhtari, H., Courtaud, B., Moyer, B. A., and Chagnes, A. (2014). Recovery of uranium from wet phosphoric acid by solvent extraction processes. *Chem. Rev.* 114, 12002–12023. doi: 10.1021/cr5001546

Comarmond, M. J., Payne, T. E., Harrison, J. J., Thiruvoth, S., Wong, H. K., Aughterson, R. D., et al. (2011). Uranium Sorption on Various Forms of Titanium Dioxide – Influence of Surface Area, Surface Charge, and Impurities. *Environ. Sci. Technol.* 45, 5536–5542. doi: 10.1021/es201046x

El-Maghrabi, H. H., Abdelmaged, S. M., Nada, A. A., Zahran, F., El-Wahab, S. A., Yahea, D., et al. (2017). Magnetic graphene based nanocomposite for uranium scavenging. *J. Hazard. Mater* 322, 370–379. doi: 10.1016/j.jhazmat.2016.10.007

El-sherif, R. M., Lasheen, T. A., and Jebril, E. A. (2017). Fabrication and characterization of CeO2-TiO2-Fe2O3 magnetic nanoparticles for rapid removal of uranium ions from industrial waste solutions. *J. Mol. Liq* 241, 260–269. doi: 10.1016/j.molliq.2017.05.119

Freundlich, H. M. F. (1906). Over the adsorption in solution. *J. Phys. Chem* 57, 385–471.

Ho, Y.-S. (2006). Review of second-order models for adsorption systems. *J. Hazard. Mater* 136, 681–689. doi: 10.1016/j.jhazmat.2005.12.043

Ho, Y. S., and McKay, G. (1999). Pseudo-second order model for sorption processes. *Process Biochem* 34, 451–465. doi: 10.1016/S0032-9592(98)00112-5

Ho, Y. S., and McKay, G. (2000). The kinetics of sorption of divalent metal ions onto sphagnum moss peat. *Water Res* 34, 735–742. doi: 10.1016/S0043-1354(99)00232-8

Kamari, A., Ngah, W. S. W., Chong, M. Y., and Cheah, M. L. (2009). Sorption of acid dyes onto GLA and H2SO4 cross-linked chitosan beads. *Desalination* 249, 1180–1189. doi: 10.1016/j.desal.2009.04.010

Karami, A., Karimyan, K., Davoodi, R., Karimaei, M., Sharafie, K., Rahimi, S., et al. (2017). Application of response surface methodology for statistical analysis, modeling, and optimization of malachite green removal from aqueous solutions by manganese-modified pumice adsorbent. *Desalin. Water Treat.* 89, 150–161. doi: 10.5004/dwt.2017.21366

Kurttio, P., Harmoinen, A., Saha, H., Salonen, L., Karpas, Z., Komulainen, H., et al. (2006). Kidney Toxicity of Ingested Uranium From Drinking Water. *Am. J. Kidney. Dis* 47, 972–982. doi: 10.1053/j.ajkd.2006.03.002

Lamb, A. C. M., Grieser, F., and Healy, T. W. (2016). The adsorption of uranium (VI) onto colloidal TiO2. *SiO2 and carbon black. Colloid Surf. A-Physicochem. Eng. Asp*. 499, 156–162. doi: 10.1016/j.colsurfa.2016.04.003

Langmuir, I. (1918). The Adsorption of Gases on Plane Surfaces of Glass, Mica and Platinum. *J. Am. Chem. Soc.* 40, 1361–1403. doi: 10.1021/ja02242a004

Li, P., Zhun, B., Wang, X., Liao, P., Wang, G., Wang, L., et al. (2017). Highly Efficient Interception and Precipitation of Uranium(VI) from Aqueous Solution by Iron-Electrocoagulation Combined with Cooperative Chelation by Organic Ligands. *Environ. Sci. Technol.* 51, 14368–14378. doi: 10.1021/acs.est.7b05288

Liu, X., Pang, H., Liu, X., Li, Q., Zhang, N., Mao, L., et al. (2021). Orderly Porous Covalent Organic Frameworks-based Materials: Superior Adsorbents for Pollutants Removal from Aqueous Solutions. *The Innovation* 2, 100076. doi: 10.1016/j.xinn.2021.100076

Manigandan, P. K., and Chandar Shekar, B. (2014). Uptake of some radionuclides by woody plants growing in the rainforest of Western Ghats in India. *J. Environ. Radioact* 130, 63–67. doi: 10.1016/j.jenvrad.2013.12.023

Nair, S., Karimzadeh, L., and Merkel, B. J. (2014). Sorption of uranyl and arsenate on SiO2, Al2O3, TiO2 and FeOOH. *Environ. Earth Sci.* 72, 3507–3512. doi: 10.1007/s12665-014-3258-x

Peng, L., Ni, Y., Wei, X., Hanyu, W., Duoqiang, P., and Wangsuo, W. (2017). Removal of U(VI) from aqueous solution using TiO2modified β-zeolite. *Radiochim. Acta* 105, 1005–1013. doi: 10.1515/ract-2017-2765

Prat, O., Vercouter, T., Ansoborlo, E., Fichet, P., Perret, P., Kurttio, P., et al. (2009). Uranium Speciation in Drinking Water from Drilled Wells in Southern Finland and Its Potential Links to Health Effects. *Environ. Sci. Technol.* 43, 3941–3946. doi: 10.1021/es803658e

Santos, E. A., and Ladeira, A. C. Q. (2011). Recovery of Uranium from Mine Waste by Leaching with Carbonate-Based Reagents. *Environ. Sci. Technol.* 45, 3591–3597. doi: 10.1021/es2002056

Schnug, E., and Lottermoser, B. G. (2013). Fertilizer-Derived Uranium and its Threat to Human Health. *Environ. Sci. Technol.* 47, 2433–2434. doi: 10.1021/es4002357

Shi, Z., Liu, C., Zachara, J. M., Wang, Z., and Deng, B. (2009). Inhibition Effect of Secondary Phosphate Mineral Precipitation on Uranium Release from Contaminated Sediments. *Environ. Sci. Technol.* 43, 8344–8349. doi: 10.1021/es9021359

Song, S., Huang, S., Zhang, R., Chen, Z., Wen, T., Wang, S., et al. (2017). Simultaneous removal of U(VI) and humic acid on defective TiO2−x investigated by batch and spectroscopy techniques. *Chem. Eng. J* 325, 576–587. doi: 10.1016/j.cej.2017.05.125

Stylo, M., Alessi, D. S., Shao, P. P., Lezama-Pacheco, J. S., Bargar, J. R., and Bernier-Latmani, R. (2013). Biogeochemical Controls on the Product of Microbial U(VI) Reduction. *Environ. Sci. Technol.* 47, 12351–12358. doi: 10.1021/es402631w

Tan, L., Zhang, X., Liu, Q., Jing, X., Liu, J., Song, D., et al. (2015). Synthesis of Fe3O4@TiO2 core–shell magnetic composites for highly efficient sorption of uranium (VI). *Colloid Surf. A-Physicochem. Eng. Asp.* 469, 279–286. doi: 10.1016/j.colsurfa.2015.01.040

Tatarchuk, T., Shyichuk, A., Mironyuk, I., and Naushad, M. (2019). A review on removal of uranium(VI) ions using titanium dioxide based sorbents. *J. Mol. Liq.* 293, 111563. doi: 10.1016/j.molliq.2019.111563

Tripathi, A., Melo, J. S., and D'souza, S. F. (2013). Uranium (VI) recovery from aqueous medium using novel floating macroporous alginate-agarose-magnetite cryobeads. *J. Hazard. Mater* 246-247, 87–95. doi: 10.1016/j.jhazmat.2012.12.002

Wang, J., He, B., Wei, X., Li, P., Liang, J., Qiang, S., et al. (2019). Sorption of uranyl ions on TiO2: Effects of pH, contact time, ionic strength, temperature and HA. *J. Environ. Sci.* 75, 115–123. doi: 10.1016/j.jes.2018.03.010

Wang, X., Fan, Q., Yu, S., Chen, Z., Ai, Y., Sun, Y., et al. (2016). RETRACTED: High sorption of U(VI) on graphene oxides studied by batch experimental and theoretical calculations. *Chem. Eng. J* 287, 448–455. doi: 10.1016/j.cej.2015.11.066

Wen, J., Li, Q., Li, H., Chen, M., Hu, S., and Cheng, H. (2018). Nano-TiO2 Imparts Amidoximated Wool Fibers with Good Antibacterial Activity and Adsorption Capacity for Uranium(VI) Recovery. *Ind. Eng. Chem. Res.* 57, 1826–1833. doi: 10.1021/acs.iecr.7b04380

Xie, Y., Chen, C., Ren, X., Wang, X., Wang, H., and Wang, X. (2019). Emerging natural and tailored materials for uranium-contaminated water treatment and environmental remediation. *Prog. Mater Sci* 103, 180–234. doi: 10.1016/j.pmatsci.2019.01.005

Xu, C., Wang, J., Yang, T., Chen, X., Liu, X., and Ding, X. (2015). Adsorption of uranium by amidoximated chitosan-grafted polyacrylonitrile, using response surface methodology. *Carbohydr. Polym* 121, 79–85. doi: 10.1016/j.carbpol.2014.12.024

Zhang, L., Zhang, L., Wu, T., Jing, X., Li, R., Liu, J., et al. (2015). In situ growth of ZnO nanorod arrays on cotton cloth for the removal of uranium(vi). *RSC Adv.* 5, 53433–53440. doi: 10.1039/c5ra08489j

Zhong, X., Liang, W., Wang, H., Xue, C., and Hu, B. (2021). Aluminum-based metal-organic frameworks (CAU-1) highly efficient UO22+ and TcO4−ions immobilization from aqueous solution. *J. Hazard. Mater* 407, 124729. doi: 10.1016/j.jhazmat.2020.124729

Zhu, K., Chen, C., Wang, H., Xie, Y., Wakeel, M., Wahid, A., et al. (2019). Gamma-ferric oxide nanoparticles decoration onto porous layered double oxide belts for efficient removal of uranyl. *J. Colloid Interface Sci* 535, 265–275. doi: 10.1016/j.jcis.2018.10.005

Conflict of Interest: The authors declare that the research was conducted in the absence of any commercial or financial relationships that could be construed as a potential conflict of interest.